

Estimation of Subsurface Structure Using Euler Deconvolution Method of Magnetic Data at the Geothermal Area of Sonai Village and its Surroundings, Konawe Regency

Sariani¹, Abdul Manan^{1*}, Bahdad², Rani Chahyani³

¹Department of Geophysical Engineering, Universitas Halu Oleo (UHO), 93232, Indonesia.

²Department of Geology Engineering, Universitas Halu Oleo (UHO), 93232, Indonesia.

³Study Program of Physics Education, Institut Agama Islam Negeri (IAIN) Kendari, 93116, Indonesia.

*Corresponding author. Email: amanan@uho.ac.id

Manuscript received: 1 August 2024; Received in revised form: 13 September 2024; Accepted: 29 October 2024

Abstract

It has been carried out research with the aim of determining the subsurface structure at the geothermal area of Sonai Village and its surroundings, Konawe Regency. The data used are magnetic data obtained through field measurements at 126 points in the N180°S direction. After the data were subjected to diurnal and IGRF corrections, a residual (local) magnetic field anomaly of around -150 nT to 90 nT was obtained. On the residual magnetic anomaly map which has been reduced to the Pole (RTP), the Euler Deconvolution (ED) method is applied to the Index Structure N=0 to estimate the subsurface structure in the form of the presence of minor faults, and it is known that there are 5 minor faults at a depth of around 9 to 38 meters. Information on the existence of these faults is then used in 2D modeling. Modeling results show that these minor faults cut through two rock layers, which are the layers composed of conglomerate rocks from the Alangga Formation and peridotites as bedrock from the Ultramafic Complex. One of the minor faults closest to the manifestation area (hot spring) is at coordinates around 4°1'12.412" S and 122°7'24.263" E to 4°1'15.532" S and 122°7'19.561" E with a distance of ±15 meters. The existence of these minor faults is thought to be the migration routes for heat flow or conduction to the surface at the geothermal area of Sonai Village and its surroundings.

Keywords: ED method; minor faults; Residual magnetic field; RTP.

Citation: Sariani, S., Manan, A., Bahdad, & Chahyani, R. (2024). Estimation of subsurface structure using Euler Deconvolution method of magnetic data at the geothermal area of Sonai Village and its surroundings, Konawe Regency. *Jurnal Geocelebes*, 8(2): 162–177, doi: 10.70561/geocelebes.v8i2.36380

Introduction

Based on geological environmental conditions, geothermal systems in Indonesia are divided into two, which are volcanic geological environments and non-volcanic geological environments. The islands of Sumatera, Java, Bali, West Nusa Tenggara, East Nusa Tenggara, Sulawesi and Maluku are areas on the volcanic geothermal route. Meanwhile, non-volcanic environments are in the areas of Bangka Belitung, West Kalimantan, South Sulawesi, Southeast Sulawesi, Central Sulawesi, Maluku and Papua (Aulia et al., 2022). For non-volcanic geothermal, it is

usually related to the presence of geological structures such as faults in the subsurface (Risdiyanto et al., 2015).

Southeast Sulawesi has the potential to have geothermal areas spread from mainland Sulawesi to Buton Island. One of the areas in Southeast Sulawesi that has geothermal potential is at Sonai Village, Puriala District, Konawe Regency.

Geothermal is a natural resource in the form of hot fluid or steam that is formed in the earth's reservoir by heating water beneath the surface by hot rocks. Heat delivery occurs in the upper mantle and earth's crust then is delivered from a heat

source to a heat reservoir on the surface. In a geothermal system there are several things that control it, including heat sources, reservoir rocks, the presence of geological structures such as faults, and water catchment areas (Suryadi et al., 2017).

In 2015, the Ministry of Energy and Mineral Resources' Geological Agency conducted a preliminary geochemical survey at the geothermal area of Puriala District (Anonymous, 2017), and found that the hot spring pH was 7 (neutral). Then Baskara (2020) researched the distribution of hot fluid at the Sonai manifestation area using the geoelectric resistivity method of the Wenner-Schlumberger configuration, and it was found that the flow of hot fluid at this area is thought to be controlled by minor faults.

In this research, the method used is the magnetic method. The magnetic method is a geophysical method that measures variations in the magnetic field on the earth's surface caused by variations in the distribution of magnetized objects beneath the earth's surface (Utama et al., 2016). Magnetic methods can also be used to determine geological structures such as faults, folds and igneous rock intrusions (Ngoh et al., 2017).

In processing magnetic data, the Euler deconvolution method (Cooper, 2024; Daniel & Kingsley, 2020) can be used to make it easier to identify the presence of geological structures, especially to determine the existence of faults in the subsurface. This method is applied to magnetic data that has undergone corrections.

Several researches using magnetic method related to geothermal have been carried out in several locations, including by Luthfin & Jubaidah (2023) at the Banyu Biru hot spring Nganjuk Regency, Lestari et al. (2022) at Air Putih Tourism Area

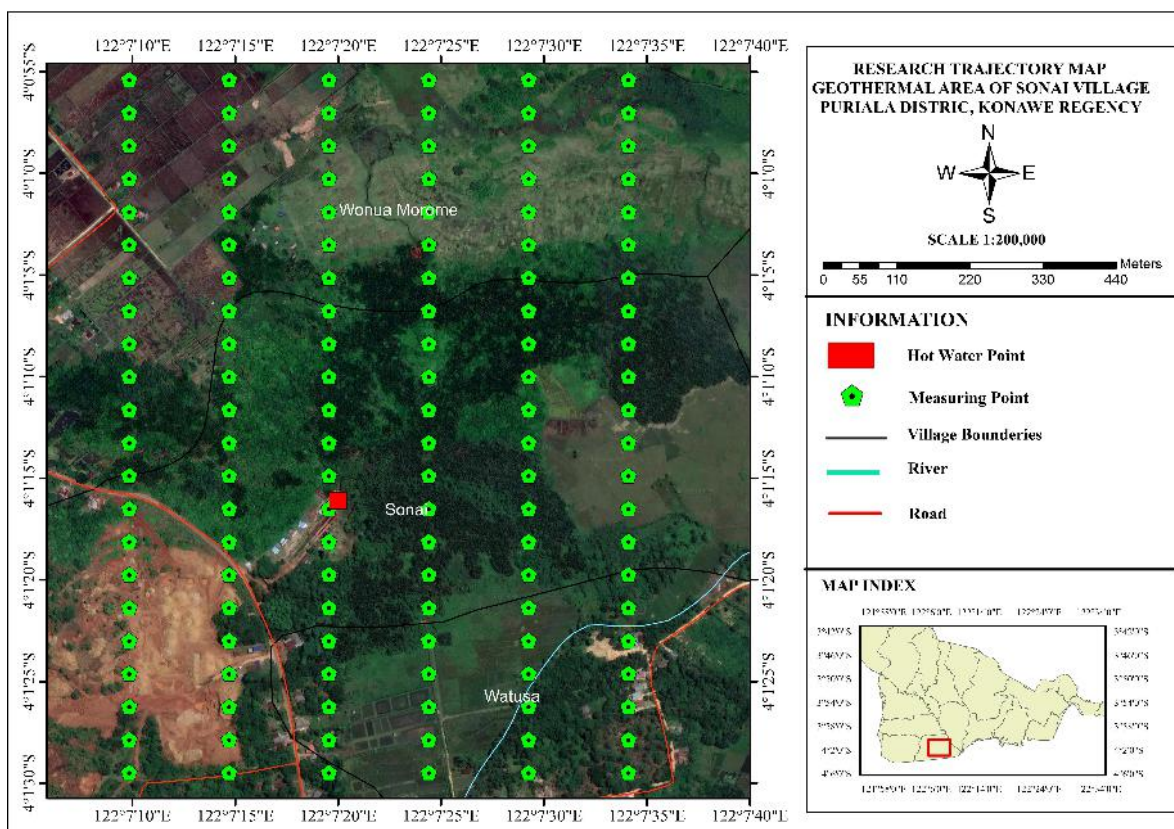
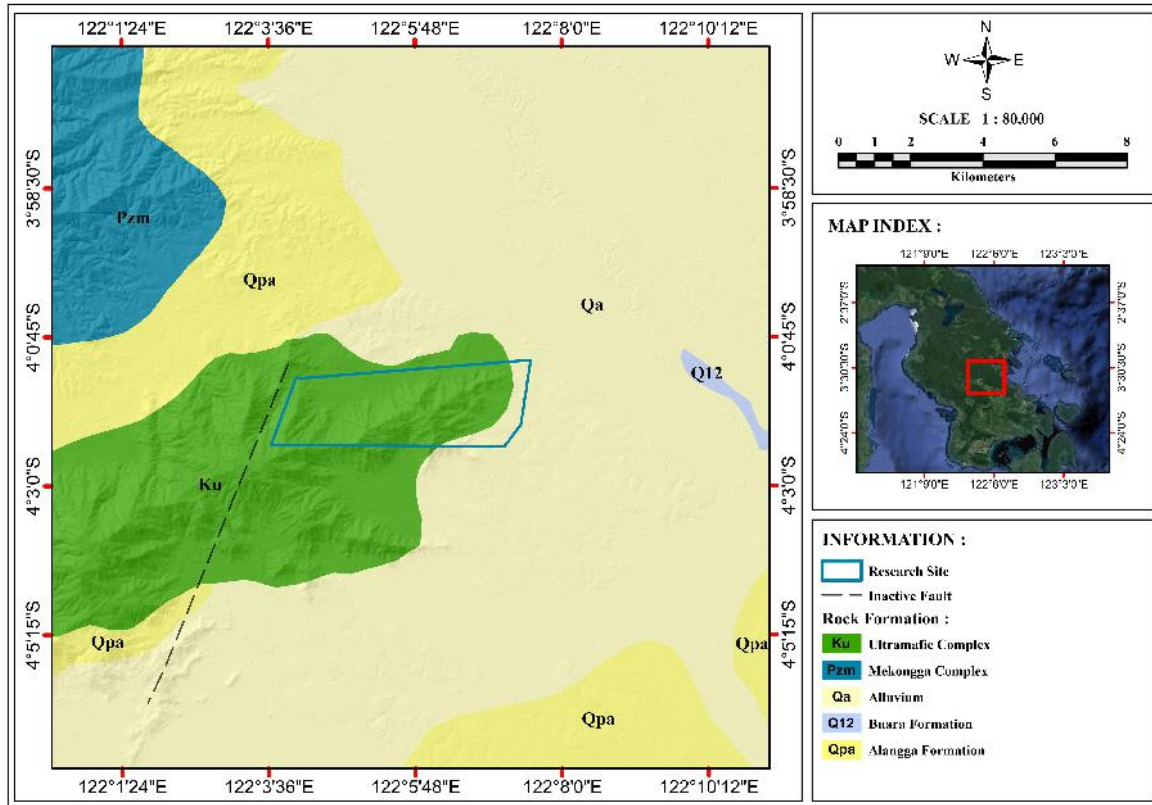
Lebong Regency, Hidayat et al. (2021) at Aie Angek Village Tanah Datar Regency, Nurhidayah (2019) at Awang Bangkal Village South Kalimantan, Sitorus & Tampubolon (2018) at the Tinggi Raja Area Simalungun Regency, Efendi et al. (2018) at the Bada Valley Central Sulawesi, Fatimah et al. (2017) at Gedong Songo Central Java, and Lestari et al. (2016) at Karangrejo Village Pacitan District. The results of these studies show that the magnetic method is able to provide adequate information regarding subsurface conditions, both layers and geological structures.

Materials and Methods

Regional Geology of the Puriala Area

Regionally, Puriala District is included in the Kolaka Series geological map (Simandjuntak et al., 1993). Based on the rock set and its characteristics, geology maps of Kolaka Series can be divided into two geological lanes, which are the Tinodo Lane and the Hialu Lane. The rocks found in the Tinodo Lane which are the base rocks are Paleozoic Metamorphic Rocks (Pzm) and are thought to be of Carboniferous age, consisting of mica schist, quartz schist, chlorite schist, graphite mica schist, slate and gneiss. The rocks found in the Hialu Lane are Ophiolite (Ku) rocks which consist of peridotite, harzburgite, dunite and serpentinite. The youngest rock on this series is Alluvium (Qa) which consists of river, swamp, and beach sediments (Zakaria & Sidarto, 2015).

Based on the regional geological map, the research area is in the central part of the Southeast Arm of Sulawesi which is still influenced by the Konaweha fault which trends Northwest-Southeast. The formations in the research area based on Figure 1 are Alluvium Sediment, Alangga Formation and Ultramafic Complex.



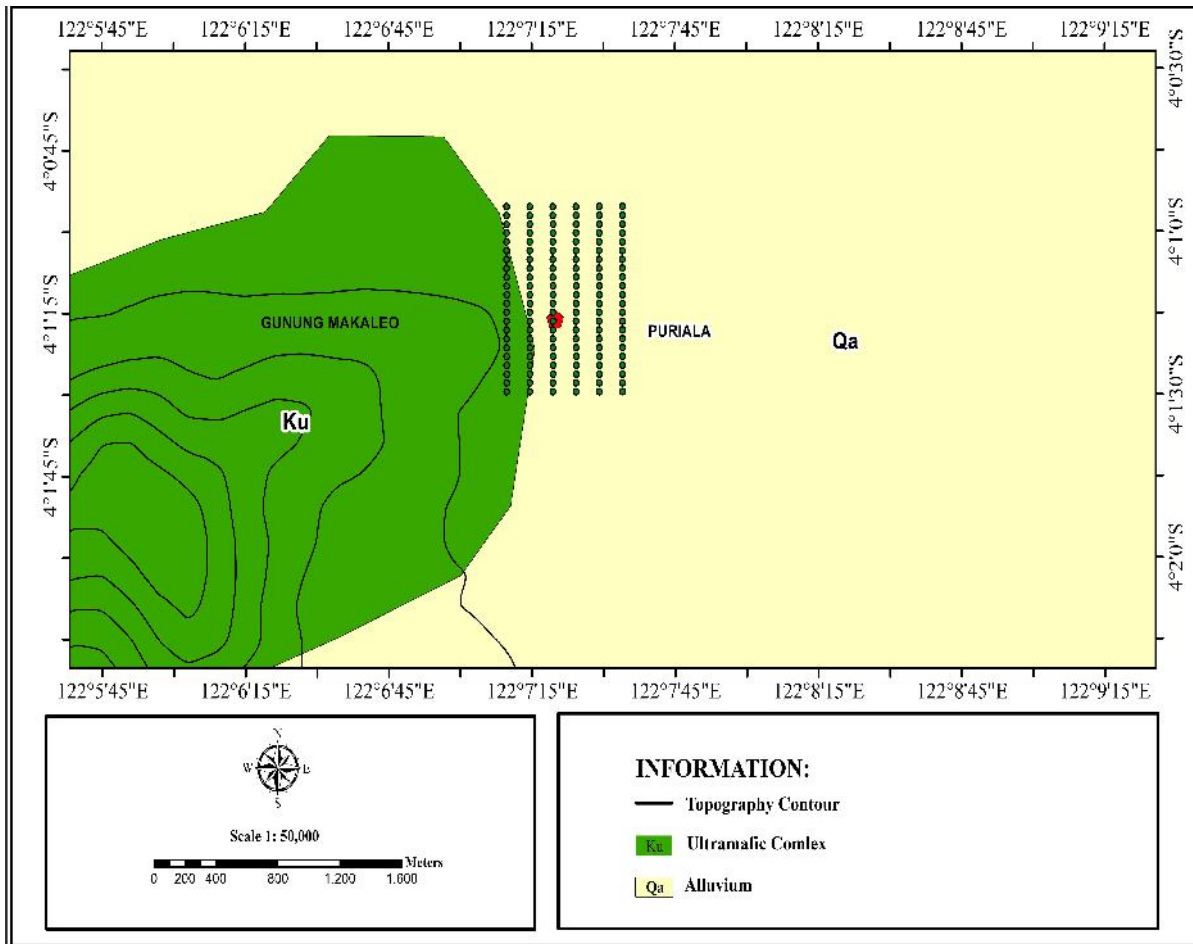


Figure 3. Research setting on geological map.

Research Setting

This research has used magnetic data as primary data. Data collection in the field was carried out using 1 set of Proton Magnetometer and Gradiometer (PMG)-2 equipment from 12 to 13 November 2023 at the geothermal area of Sonai Village and its surroundings, Puriala District, Konawe Regency. The number of measurement points is 126 points with a distance of ±50 meters on 6 trajectories in the direction of N180°S. The area of the research is approximately 1,050×900 meters. The research setting map can be seen in Figure 2 and the research setting map on the geological map can be seen in Figure 3. Apart from that, secondary data was also used in the form of an inclination angle of -23.75° and a declination of 0.36° at the research location.

Data Processing

1. Diurnal Correction

Diurnal Correction is a correction made to magnetic field data measured in the field to eliminate the influence of external magnetic fields or diurnal variations. Calculation of Diurnal Correction is carried out using the formula (Telford et al., 1990):

$$d = \left(\frac{H_1 - H_0}{t_1 - t_0} \right) (t_n - t_0) \quad (1)$$

with H_d is the Diurnal Variation Correction, H_1 is the magnetic field value at the end point, H_0 is the magnetic field value at the starting point, t_0 is the measurement time at the starting point, t_1 is the measurement time at the end point, and t_n is the measurement time at point n .

2. IGRF Correction

IGRF (International Geomagnetic Reference Field) correction is a correction made to measured magnetic field data that has been corrected for diurnal variations to remove the influence of the Earth's main magnetic field. IGRF values for the research area were obtained from The International Association of Geomagnetism and Aeronomy (IAGA) via www.ngdc.noaa.gov/. IGRF correction is calculated using the formula (Sirait, 2021; Utama et al., 2016):

$$H_t = H_d \pm H_{dv} - H_o \quad (2)$$

where H_t is the total magnetic field anomaly, H_d is the H value at each measurement point, H_{dv} is the Diurnal Variation Correction, and H_o is the IGRF correction for the Sonai village geothermal area and its surroundings.

3. Upward Continuation

After performing the two corrections above, the total magnetic anomaly data is then transformed using Upward Continuation ($H_{\text{continuation}}$). This stage functions to separate regional magnetic field anomalies from total magnetic field anomalies (Kamureyina et al., 2019; Setiani et al., 2019; Pancasari et al., 2020). In Fikar et al. (2019) it is stated that this process is to eliminate local influences originating from surface sources and clarify the influence of regional magnetic field anomalies.

4. Residual Magnetic Field Anomaly

In this research, the target is the residual (local) magnetic field anomaly. The anomaly is obtained following the equation (Telford et al., 1990):

$$H_l = H_t - H_{\text{continuation}} \quad (3)$$

where H_l is the residual magnetic field anomaly, H_t is the total magnetic anomaly and $H_{\text{continuation}}$ is the magnetic anomaly resulting from Upward Continuation.

5. Reduction to Pole (RTP)

The residual magnetic field anomaly data that has been obtained is then carried out by the RTP process on it. It is hoped that the magnetic field anomaly is located directly above the body of the object causing the anomaly. This transformation process changes dipole magnetic anomaly data into monopole data (Sehah et al., 2023).

6. Euler Deconvolution Method

The Euler Deconvolution method is used to estimate the location and depth of anomaly sources in the subsurface (Ghanbarifar et al., 2024; Cooper, 2024), especially the presence of minor faults.

The Euler Deconvolution method is based on the degree of Euler homogeneity which is interpreted as the Index Structure (N). The Index Structure for several anomaly models can be seen in Table 1 (Stavrev and Reid, 2007). The Euler Deconvolution equation at (x,y,z) coordinate is (Pham et al., 2024; Daniel & Kingsley, 2020):

$$\left(\frac{\partial}{\partial x} \right)^N + \left(\frac{\partial}{\partial y} \right)^N + \left(\frac{\partial}{\partial z} \right)^N = N(B-H) \quad (4)$$

where (x, y, z) is the coordinate of the anomaly source, H the total magnetic field detected at (x, y, z) , and B the regional magnetic field.

Table 1. Index Structure (N) for several magnetic anomaly models (Stavrev & Reid, 2007).

N	Magnetic Anomaly Model
0	Contact/ fault
1	Sill/ dike
2	Cylinder

Results and Discussion

The Total Magnetic Field Measured at the Research Area

Magnetic field measurements at the Sonai geothermal area and its surroundings were carried out using 1 set of PMG-2 equipment. The measurement results are in the form of uncorrected magnetic anomaly

contour as shown in Figure 4. The magnetic field values obtained ranged from 42,220.59 nT to 42,469.21 nT.

Figure 4 shows that there are tighter and looser contour closures. This situation is

caused by the inhomogeneous distribution of the magnetic susceptibility of the material or layer in the subsurface.

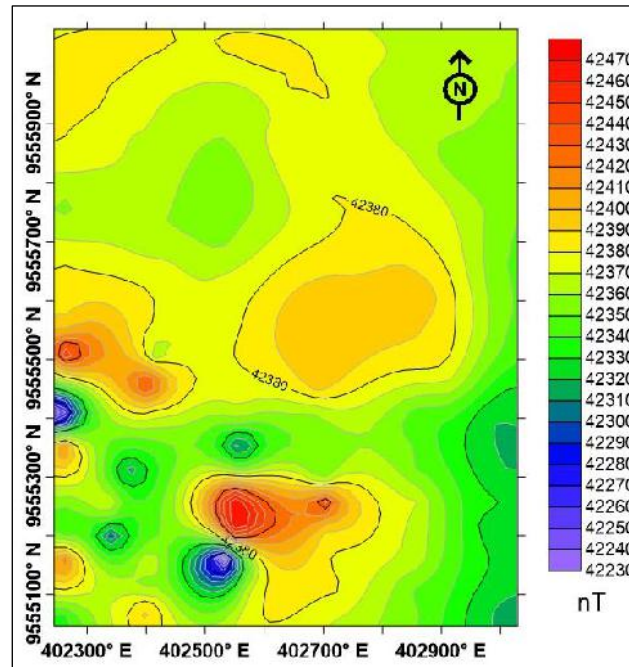


Figure 4. Measured magnetic field distribution.

Total Magnetic Field Anomaly

The total magnetic field anomaly value in an area can be calculated using equation (4). After performing Diurnal and IGRF Corrections, it is known that the magnetic anomaly values at the research area are between -171.17 nT and 82.47 nT. This result can be seen in Figure 5.

Based on Figure 5, qualitatively the distribution of total magnetic field anomalies in the research area is divided into three different anomaly trends, which are high, medium, and low anomalies. The distribution of high anomalies with an anomaly range of around 10 nT to 82 nT is dominant in the Northern part with a West-Northeast direction. The distribution of this anomaly pattern decreases towards the West. The medium anomaly pattern with an anomaly range of around -90 nT to 10 nT is in the Southern part of the research area. This medium anomaly has a

downward trend from North-Northwest to West-Northwest. Meanwhile, the low anomaly pattern with an anomaly range of around -171 nT to -90 nT is dominant in the South-Southwestern part of the research area.

Upward Continuation Results

Through a trial-and-error process, Upward Continuation was carried out 6 times, which are at a height of 150 meters, 200 meters, 250 meters, 300 meters, 350 meters, and 400 meters, and the results are shown in Figure 6. Based on the contour map, it can be seen that the lifting process stopped at a height of 300 meters because at this height the shallow anomalies tended to disappear leaving regional anomalies as marked with contour changes that tend to stabilize if the lifting process continues at a higher level.

Residual Magnetic Field Anomaly

The results of Upward Continuation are still in the form of regional magnetic field anomalies which are not the research target, so to obtain residual (local)

magnetic anomalies which are the target, further processing needs to be carried out. Residual anomaly follows equation (3).

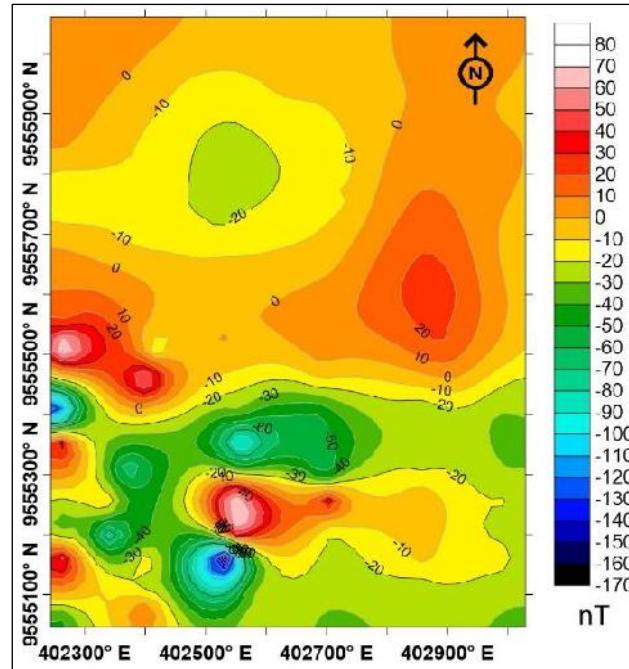


Figure 5. Corrected total magnetic field anomaly distribution.

The residual magnetic field anomaly contour map in Figure 7 shows the local geological structure pattern in the research area. This figure shows qualitatively the distribution of areas with high and low susceptibility values. The residual magnetic field anomaly contour ranges from -150 nT to 90 nT where medium to high anomalies is in the Northern part of the research area and low anomaly contours are dominant in the Southern part.

RTP Transformation of Residual Magnetic Anomaly Data

The residual magnetic field anomaly data are then subjected to RTP transformation with the aim of eliminating the influence of the magnetic inclination angle. In this research, the transformation was carried out from inclination -23.75° to 90° and from declination 0.36° to 0° . This transformation is performed on the residual magnetic field anomaly data. The

results ranged from around -89.1 nT to 91 nT which can be seen in Figure 8.

Applying Euler Deconvolution Method to Residual Anomaly Contour Map

The application of Euler Deconvolution method begins with creating a synthetic fault model which is then tested for the Euler Deconvolution response. Subsurface geological structures, especially the location and depth of faults, are identified based on the use of the Index Structure $N=0$ with a maximum error tolerance of 15%.

The results of Euler Deconvolution can be seen in Figure 9. Based on this figure, several minor faults were found at the research location. The suspected location of minor faults is marked by a distribution of green and blue Euler points. The location is in the North-East which stretches to the Southeast, as well as in the North to North-West. A small number of faults are also in the South and Southwest,

close to area of geothermal manifestation (hot spring). These minor faults are a

depth of around 9 to 38 meters.

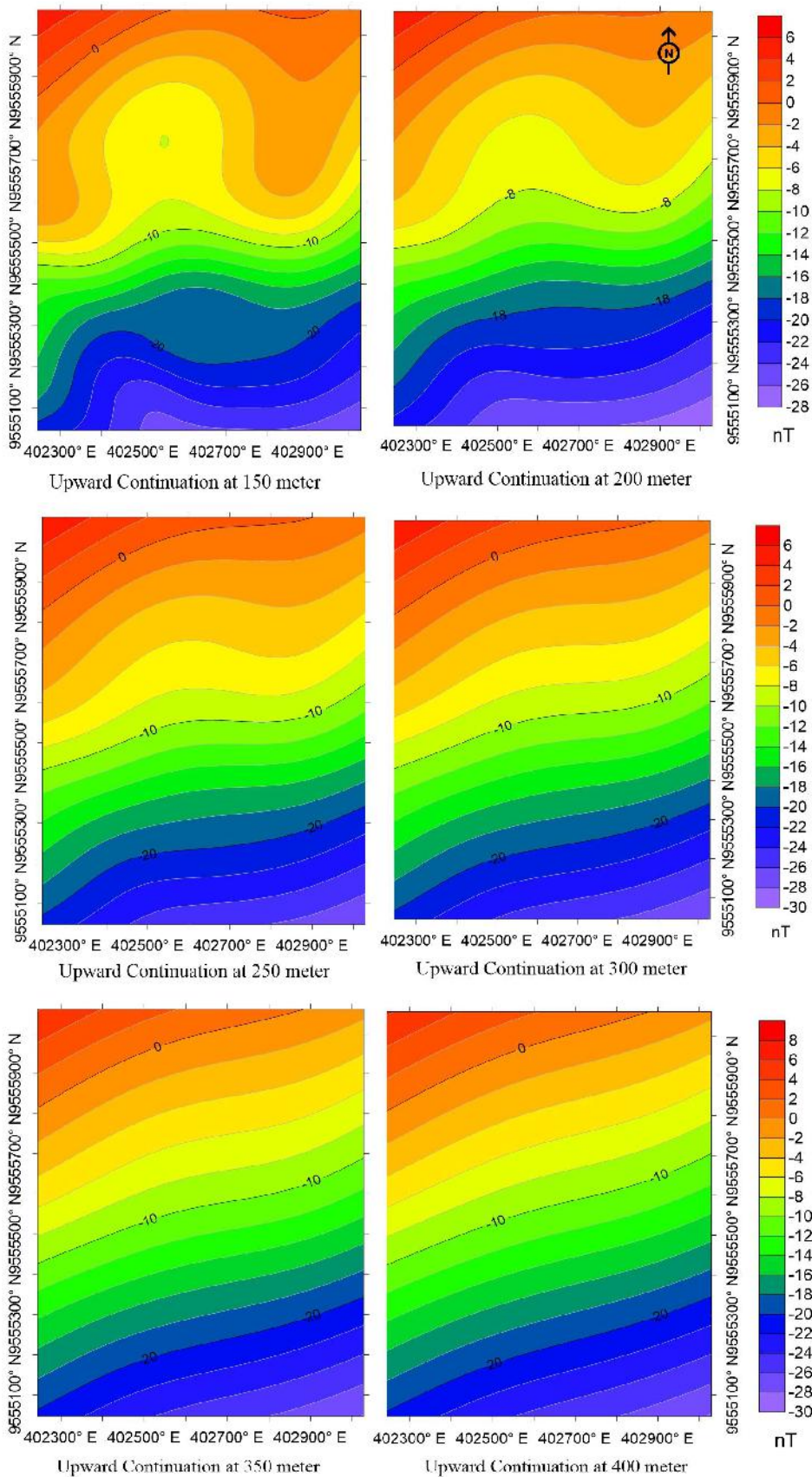


Figure 6. Upward continuation at a height of 150 to 400 meters.

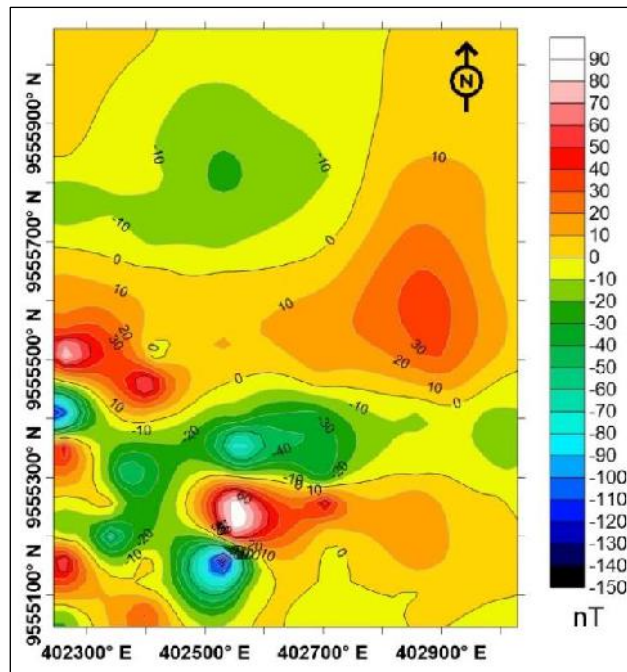


Figure 7. Residual magnetic field anomaly distribution.

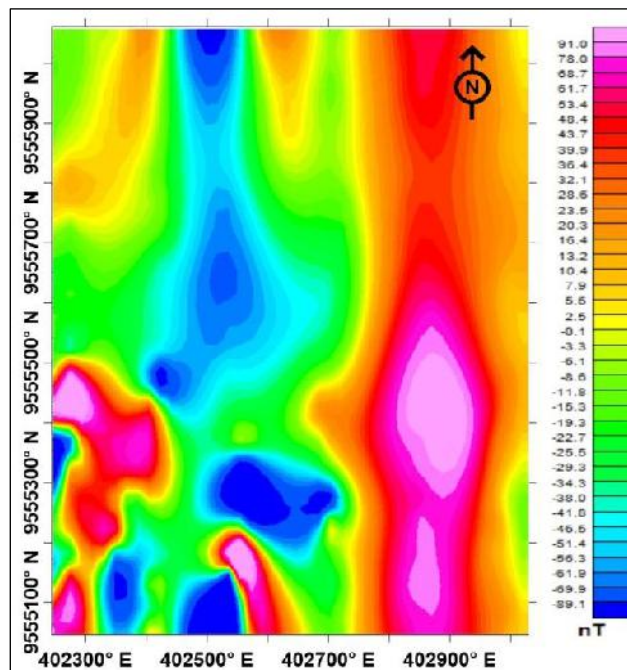


Figure 8. Residual magnetic anomaly contour that has been reduced to the Pole (RTP).

Making Slices for 2D Modeling

For 2D modeling, 2 slices were made on the residual magnetic anomaly map. These slices are A-A' and B-B' (Figure 10). For the first slice or A-A' slice, it is transverse from the North-West to the Southeast through areas where 3 minor faults are thought to lie in the subsurface. Meanwhile, the second slice or B-B' slice runs transversely from West to East

through the geothermal manifestation (hot spring), as well as through areas where it is suspected that there are also 3 faults in the subsurface. Determining the slice paths is based on the result of Euler Deconvolution, so it will be easier to determine the presence of faults through 2D subsurface modeling.

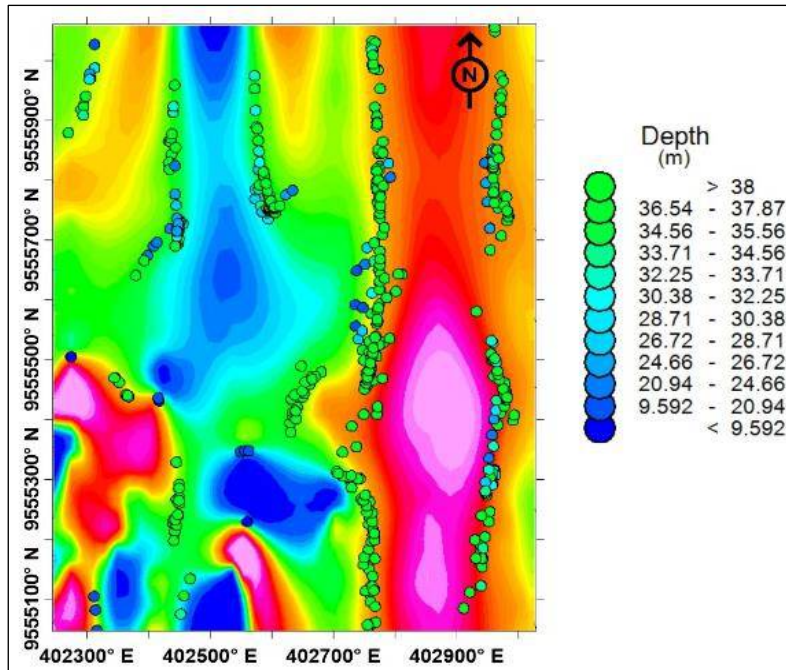


Figure 9. Euler points on the residual magnetic anomaly contour.

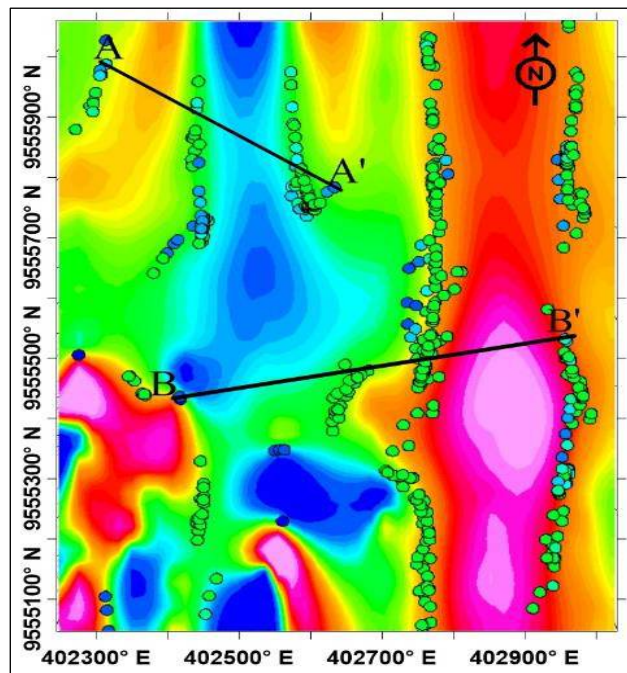


Figure 10. Direction of A-A' and B-B' slices.

2D Modeling Results of Subsurface Structure

Based on the result of 2D modeling for the A-A' slice in Figure 11, it was found that the subsurface condition consists of three layers, which are the first layer consists of three types of rocks with a susceptibility value of 0.001 which is thought to be sand, a susceptibility value of 0.002 is thought to be clay and 0.004 as sandstone. Sand and

clay are included in the Alluvium Sediment which is characterized by the presence of swamps near the geothermal manifestation area, while sandstone is included in the Alangga Formation. The second layer consists of only one type of rock, which is rock with a susceptibility value of 0.005 which is thought to be conglomerate rock, and from the figure it looks relatively dominant in the Northwest

part of the research area. This rock is included in the Alangga Formation. Meanwhile, the third layer is only composed of rocks with a susceptibility

value of 0.01 which is thought to be peridotite and is included in the Ultramafic Complex. This layer is relatively thinner in the Southeast of the research area.

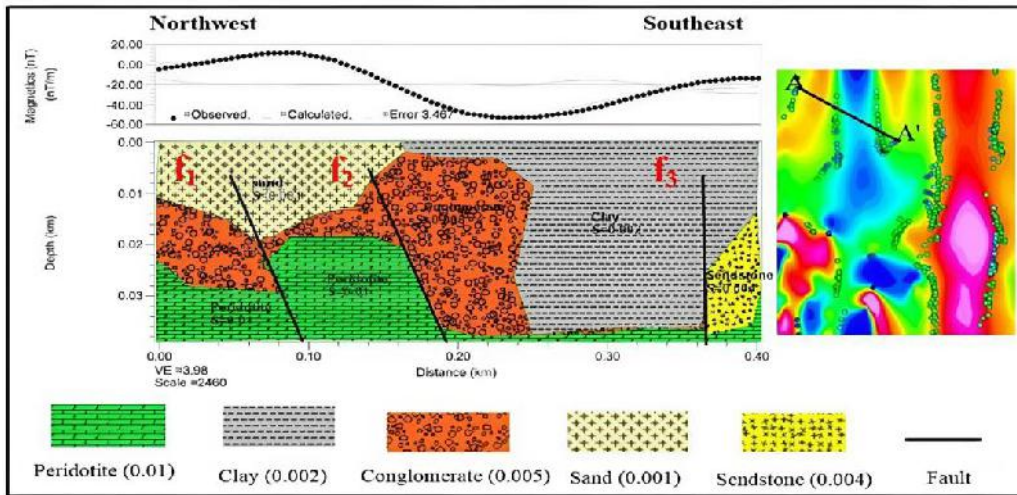


Figure 11. 2D modeling result for A-A' slice.

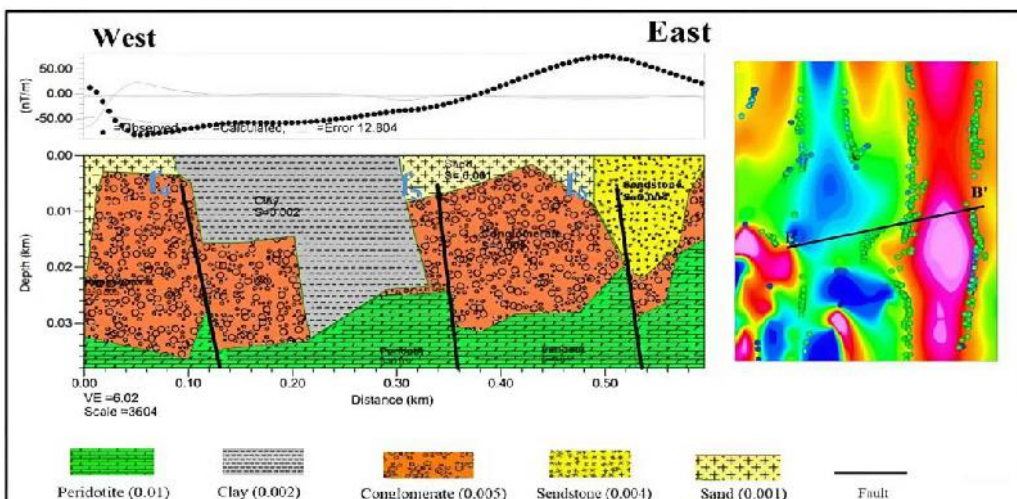


Figure 12. 2D modeling result for B-B' slice.

For the B-B slice in Figure 12, three layers were also found. The first layer consists of three types of rocks with each susceptibility value of 0.001 which is thought to be sand, 0.002 which is thought to be clay and 0.004 which is thought to be sandstone. The first two types of rocks are the Alluvium Sediments, while the third is included in the Alangga Formation. The second layer consists only of rocks with a susceptibility value of 0.004 which is thought to be conglomerate rock, and includes the Alangga Formation. Meanwhile, the third layer also consists of only one type of rock, which is rock with a

susceptibility value of 0.01, and is thought to be peridotite. This rock is part of the Ultramafic Complex. It can be seen that the thickness of this rock layer is relatively thicker than the peridotite layer in the A-A slice.

The rocks or materials found through modeling are in accordance with the regional geological map of the research area in Figure 1. In addition, it is also in accordance with the geological conditions found directly in the research area where swamps and peridotite outcrops were found which can be seen in Figure 13.



Figure 13. (a). Alluvium sediments in the form of swamps, (b). Laterite soil, and (c). Weathered peridotite outcrop.

The first layer in Figures 11 and 12 above is a layer that can function as a fluid reservoir in geothermal area. This is because alluvium sediments such as sand and clay are loose materials and have pores that are good enough to store and pass water. It is this permeable nature that allows this layer to become a reservoir zone. The second layer is also a permeable layer because it is formed from conglomerate and sandstone from the Alangga Formation. While the third layer is a compact layer formed from peridotite. Peridotite is an igneous rock from the Ultramafic Complex that can function as a bedrock layer. This is because of its impermeable nature.

In this research, several minor fault segments were also found, as can be seen in Figures 11 and 12 above. Minor faults were found at 6 different locations, which are:

1. Fault f_1 is located at coordinates $4^{\circ}0'61.041''$ S and $122^{\circ}7'16.172''$ E to $4^{\circ}1'5.421''$ S and $122^{\circ}7'15.411''$ E, and is approximately 363 meters from the hot spring.
2. Fault f_2 is located at coordinates $4^{\circ}1'2.360''$ S and $122^{\circ}7'14.110''$ E to $4^{\circ}1'12.168''$ S and $122^{\circ}7'15.061''$ E, and is approximately 68 meters from the hot spring.
3. Fault f_3 is at coordinates $4^{\circ}1'22.051''$ S and $122^{\circ}7'19.232''$ E to $4^{\circ}1'9.371''$ S

and $122^{\circ}7'19.640''$ E, and is approximately 30 meters from the hot spring.

4. Fault f_4 is at coordinates $4^{\circ}1'18.345''$ S and $122^{\circ}7'13.177''$ E to $4^{\circ}1'27.255''$ S and $122^{\circ}7'17.363''$ E, and is approximately 32 meters from the hot spring.
5. Fault f_5 is at coordinates $4^{\circ}1'12.412''$ S and $122^{\circ}7'24.263''$ E to $4^{\circ}1'15.532''$ S and $122^{\circ}7'19.561''$ E, and is approximately 15 meters from the hot spring.
6. Fault f_6 is at coordinates $4^{\circ}1'17.610''$ S and $122^{\circ}7'27.189''$ E to $4^{\circ}1'27.431''$ S and $122^{\circ}7'35.240''$ E, and is approximately 57 meters from the hot spring.

Regionally, the research area is influenced by the Konaweha strike-slip fault which trends Northwest-Southeast (Tamburaka, 2019). As a result of this fault shift, minor faults were formed which caused the emergence of manifestation such as hot spring in the research area. This fault was formed based on the deformation relationship between the horizontal fault system and the formation of a basin called a pull-apart-basin so that the conglomerate layer in the Northwest (NW) and Southeast (SE) of the research area tends to be thinner than the conglomerate layer in the middle.

The minor faults found in this research cut through the Alangga Formation and bedrock layer as shown in Figures 11 and 12. This condition shows that the type of geothermal at Sonai Village and its surroundings is non-volcanic geothermal where the fluid comes from surface water, and the heat source is controlled by fractures in the form of minor faults formed in the rocks. The fracture zone is a permeable zone that is capable of channeling geothermal fluid.

The fault zones in Figures 11 and 12 are thought to act as geothermal fluid migration routes to the surface. As a result of these zones, fluid is heated and moves upwards so that it accumulates in the permeable zone (alluvium sediment). The movement of the fluid is thought to also be influenced by the topography of the research area where fluid originating from surface water will move and accumulate in lower area. Because the area is close to minor fault zones, hot spring emerges in the area. The area in question is now known by the local population as the Sonai hot spring, Puriala.

Conclusion

Based on the research results, it can be concluded that the Sonai area and its surroundings are composed of 3 formations, which are Alluvium Sediment, Alangga Formation and Ultramafic Complex. For Alluvium Sediment, it was found to be sand with a susceptibility value of 0.001 and clay with a susceptibility value of 0.002. For the Alangga Formation, it consists of sandstone with a susceptibility value of 0.004 and conglomerate rock with a susceptibility value of 0.005. Meanwhile, the Ultramafic Complex consists of peridotite rock with a susceptibility value of 0.001.

Apart from that, in the research area geological structures were found in the

form of minor faults at a depth of around 9 to 38 meters which are thought to be the cause of the emergence of geothermal manifestation such as hot spring. Of the several faults found, one of the minor faults closest to the manifestation is at coordinates $4^{\circ}1'12.412''$ S and $122^{\circ}7'24.263''$ E to $4^{\circ}1'15.532''$ S and $122^{\circ}7'19.561''$ E with a distance of ± 15 meters. The formation of these faults is thought to be caused by the activity of the Konaweha fault which is close to the manifestation area. These minor faults cut through two rock layers, which are a layer composed of conglomerate rock from the Alangga Formation and a rock layer composed of peridotite from the Ultramafic Complex. This peridotite layer functions as bedrock at the Sonai geothermal area, Puriala District, Konawe Regency.

The existence of minor faults found at the area Sonai geothermal is thought to be the pathways of geothermal migration to the surface through conglomerate rock and peridotite layers, both in the form of heat flow and conduction. These minor faults act as heat controllers. At the same time, it proves that the type of geothermal in this area is non-volcanic.

Acknowledgements

Thank you to all parties who have helped this research, especially to the Geophysical Engineering Laboratory that has allowed the use of PMG-2 equipment for data acquisition in the field, laboratory assistants and friends of the magnetic-geothermal research team who have worked together in collecting data in the field.

Author Contribution

In compiling this research article, each author is divided into several job desks. The one responsible for procuring literatures, collecting and processing data

is Sariani, while the design of the research survey and preparation of the article are done by Rani Chahyani. The supervisors and observers in the research and writing of this article are Abdul Manan and Bahdad.

Conflict of Interest

We declare that there is no conflict of interest in the preparation and publication of this paper.

References

- Anonymous. (2017). *Potensi Panas Bumi Indonesia Jilid 2*. Direktorat Panas Bumi, Kementerian Energi dan Sumber Daya Mineral.
- Aulia, R. N., Nur, I., & Ilyas, A. (2022). Karakteristik Fluida Panas Bumi Berdasarkan Analisis Geokimia Air Panas Wawolesea Kabupaten Konawe Utara Sulawesi Tenggara. *Jurnal Gecelebes*, 6(1), 64–71. <https://doi.org/10.20956/gecelebes.v6i1.19672>
- Baskara, M. Y. (2020). *Identifikasi Sebaran Fluida Panas Daerah Panasbumi Puriala, Kabupaten Konawe Menggunakan Metode Geolistrik Resistivitas Konfigurasi Wenner Schlumberger*. Universitas Halu Oleo.
- Cooper, G. R. J. (2024). Using Euler Deconvolution as Part of a Mineral Exploration Project. *Minerals*, 14(4), 393. <https://doi.org/10.3390/min14040393>
- Daniel, O. B., & Kingsley, K. T. (2020). Application of 3D Euler Deconvolution and 2D Inverse Modelling to Basin Depth Estimation, the Case of the Keta Basin, Ghana. *NRIAG Journal of Astronomy and Geophysics*, 9(1), 393–401. <https://doi.org/10.1080/20909977.2020.1743019>
- Efendi, R., Fazri, M., Rusydi, H., & Kasim, S. (2018). Interpretasi Data Magnetik Menggunakan Dekonvolusi Euler, Studi Kasus: Lembah Bada Poso Sulawesi Tengah. *Jurnal Geosains Kutai Basin*, 1(1), 1–5. <https://jurnal.fmipa.unmul.ac.id/index.php/geofis/article/view/169>
- Fatimah, F., Lavanto, T. A., Gunawan, B., & Febriarto, O. (2017). Analisis Potensi Panas Bumi dengan Metode Geomagnetik di Daerah Gedong Songo Ungaran Jawa Tengah. *KURVATEK*, 2(2), 35-43.
- Fikar, M., Hamimu, L., Manan, A., & Suyanto, I. (2019). Pemodelan 2D Data Magnetik Menggunakan Transformasi RTP untuk Pendugaan Sesar di Daerah Kasihan, Pacitan, Jawa Timur. *Jurnal Rekayasa Geofisika Indonesia (JRGI)*, 01(02), 33–42. <https://ojs.uho.ac.id/index.php/jrgi/article/view/8721>
- Ghanbarifar, S., Hosseini, S.H., Ghiasi, S.M., Abedi, M., & Afshar, A. (2024). Joint Euler Deconvolution for Depth Estimation of Potential Field Magnetic and Gravity Data. *International Journal of Mining and Geo-Engineering*, 58(2), 121–134. https://ijmge.ut.ac.ir/article_95272.html
- Hidayat, H., Putra, A., & Pujiastuti, D. (2021). Identifikasi Sebaran Anomali Magnetik pada Daerah Prospek Panas Bumi Nagari Aie Angek, Kabupaten Tanah Datar. *Jurnal Fisika Unand (JFU)*, 10(1), 48-54. <https://doi.org/10.25077/jfu.10.1.48-54.2021>
- International Association of Geomagnetism and Aeronomy. *National Centers for Environmental Information*. www.ngdc.noaa.gov/.
- Kamureyina, E., Omang, B. O., Simon, K., Owolabi, A., & Nur, A. (2019). Determination of Hydrocarbon Potentials Using HighResolution Aeromagnetic Data over Sokoto Basin Northwestern Nigeria. *International Journal of Geosciences*,

- 10, 419-438.
<https://doi.org/10.4236/ijg.2019.104024>
- Lestari, S. E., Yunita, A., Rahman, R. A., Refrizon, R., & Sugianto, N. (2022). Aplikasi Metode Magnetik Pada Pemetaan Sumber Panas Bumi di Kawasan Wisata Air Putih, Lebong, Bengkulu. *Newton-Maxwell Journal of Physics*, 3(2), 71–76.
<https://doi.org/10.33369/nmj.v3i2.23125>
- Lestari, T. E., Wibowo, B.N., & Darmawan, D. (2016). Interpretasi Bawah Permukaan Daerah Manifestasi Panas Bumi Desa Karangrejo Kecamatan Arjosari Pacitan Menggunakan Metode Geomagnet. *Jurnal Fisika*, 5(1), 1–7.
<https://journal.student.uny.ac.id/fisika/article/view/157>
- Luthfin, A., & Jubaidah, N. A. (2023). Identification of Geothermal Distribution in The Banyu Biru Hot Water Source using The Magnetic Method. *Indonesian Journal of Applied Physics (IJAP)*, 13(2), 215–225.
<https://doi.org/10.13057/ijap.v13i2.72305>
- Ngoh, J. N., Mbarga, T. N., Assembe, S. P., Meying, A., Owono, O. U., & Tabod, T. C. (2017). Evidence of Structural Facts Inferred from Aeromagnetic Data Analysis over the Guider-Maroua Area (Northern Cameroon). *International Journal of Geosciences*, 8(6), 781–800.
<https://doi.org/10.4236/ijg.2017.86044>
- Nurhidayah, A., Wahyono, S. C., & Siregar, S. S. (2019). Interpretasi Bawah Permukaan Daerah Penambangan Batuan Andesit Awang Bangkal Kabupaten Banjar Kalimantan Selatan Menggunakan Metode Magnetik. *Jurnal Fisika Flux*, 16(2), 117–123.
<https://doi.org/10.20527/flux.v16i2.5184>
- Pancasari, A., Safani, J., & Manan, A. (2020). Interpretasi Struktur Bawah Permukaan Daerah Kota Kendari Berdasarkan Data Anomali Medan Magnetik Lokal. *Jurnal Rekayasa Geofisika Indonesia (JRGI)*, 02(2), 45–53.
- Pham, L. T., Oliveira, S. P., Abdelrahman, K., Gomez-Ortiz, D., Nguyen, D. V., Vo, Q. T., & Eldosouky, A. M. (2024). Selection of Euler Deconvolution Solutions Using the Enhanced Horizontal Gradient and Stable Vertical Differentiation. *Open Geosciences*, 16(1), 20220637.
<https://doi.org/10.1515/geo-2022-0637>
- Risdianto, D., Permana, L. A., Wibowo, A. E. A., Sugianto, A., & Hermawan, D. (2015). *Sistem Panasbumi Non-Vulkanik di Sulawesi*. Pusat Sumber Daya Geologi, Badan Geologi, Kementerian Energi dan Sumber Daya Mineral.
- Sehah, S., Prabowo, U. N., Raharjo, S. A., & Prasetya, R. I. (2023). Two-Dimensional Modeling of Magnetic Anomaly Data Reduced to the Poles in the Andesitic Prospect Area of the Southeast Slope of Slamet Volcano, Indonesia. *Earth Sciences Malaysia (ESMY)*, 7(2), 75–82.
<https://doi.org/10.26480/esmy.02.2023.75.82>
- Setiani, N., Safani, J., & Manan, A. (2019). Interpretasi Struktur Bawah Permukaan Daerah Kota Kendari Berdasarkan Data Anomali Medan Magnetik Regional. *Jurnal Rekayasa Geofisika Indonesia (JRGI)*, 03(1), 25–32.
- Simandjuntak, T. O., Suro., & Hadiwijoyo, S. (1993). *Peta Geologi Lembar Kolaka Skala 1:250.000*. Pusat Penelitian dan Pengembangan Geologi.
- Sirait, R. (2021). Analisis Anomali Magnetik dalam Penentuan Struktur Geologi dan Litologi Bawah Permukaan sebagai Manifestasi Panas

- Bumi di Panyabungan Selatan Sumatera Utara. *Jurnal Fisika Flux*, 18(2), 83–92. <https://doi.org/10.20527/flux.v18i2.7402>
- Sitorus, E., & Tampubolon, T. (2018). Penentuan Struktur Bawah Permukaan Area Panas Bumi Tinggi Raja Kabupaten Simalungun Dengan Menggunakan Metode Magnetik. *Jurnal Einstein*, 6(1), 26–33. <https://jurnal.unimed.ac.id/2012/index.php/einsten/article/view/12060>
- Stavrev, P., & Reid, A. (2007). Degrees of Homogeneity of Potential Fields and Structural Indices of Euler Deconvolution. *Geophysics*, 72(1), L1–L12. <https://doi.org/10.1190/1.2400010>
- Suryadi, S., Haerudin, N., Karyanto., & Sudrajat, Y. (2017). Identifikasi Struktur Bawah Permukaan Lapangan Panas Bumi Way Ratai Berdasarkan Data Audio Magnetotelluric (AMT). *Jurnal Geofisika Eksplorasi*, 3(1). <https://journal.eng.unila.ac.id/index.php/geo/article/view/1033>
- Tamburaka, E. (2019). Risiko dan Mitigasi Bencana Gempa Tektonik di Kabupaten Konawe. *Jurnal Aksara Publik*, 3(2), 222–235.
- Utama, W., Warnana, D. D., Bahri, S., & Hilyah, A. (2016). Eksplorasi Geomagnetik Untuk Penentuan Keberadaan Pipa Air di Bawah Permukaan Bumi. *Jurnal Geosaintek*, 2(3), 157–159. <http://dx.doi.org/10.12962/j25023659.v2i3.2099>
- Zakaria, Z., & Sidarto, S. (2015). Aktifitas Tektonik di Sulawesi dan Sekitarnya Sejak Mesozoikum Hingga Kini Sebagai Akibat Interaksi Aktifitas Tektonik Lempeng Tektonik Utama di Sekitarnya. *Jurnal Geologi dan Sumberdaya Mineral*, 16(3), 115–127. <https://jgsm.geologi.esdm.go.id/index.php/JGSM/article/view/36>